

Development of aluminum composite reinforced with selected agricultural residues

L. Osunmakinde¹ · T. B. Asafa¹ · P. O. Agboola² · M. O. Durowoju¹

Received: 17 August 2023 / Accepted: 13 December 2023

Published online: 21 December 2023

© The Author(s) 2023 [OPEN](#)

Abstract

The use of agricultural residue has been considered an economic and environmentally friendly approach for development of aluminium composites. In this study, Al powder (Al) was reinforced with coconut shell ash (CSA), rice husk ash (RHA), and cassava peel ash (CPA) for enhanced physicomaterial performance of the resulting composites. Five samples (A_0 -Al, A_1 -Al + 15RHA, A_2 -Al + 5CSA + 5RHA + 5CPA, A_3 -Al + 15CPA, and A_4 -Al + 15RHA) were prepared in a two-step stir-casting technique and characterized based on physical, mechanical and metallurgical properties. Microstructural analysis revealed that all the particles bonded well with the aluminum alloy. The densities of samples A_1 , A_2 , A_3 , and A_4 reduced by 4.78%, 7.75%, 11.44%, and 14.76%, respectively compared to the control sample A_0 while porosities rose by 2.1%, 2.23%, 2.56%, and 2.98% respectively. Sample A_2 has the highest tensile strength (39.84 MPa) and hardness (120 HBR) which denote 33.60% and 64.27% enhancement compared to the unreinforced sample. These observations can be attributed to the presence of intermetallic compounds such as Fe_3Si and Al_6Fe present in the composites as well as uniformly distributed and strongly bounded reinforcement within the aluminum matrix. The composite made from the combination of the three reinforcements gave the best physicomaterial properties and therefore recommended for engineering applications.

Keywords Composite · Agricultural residues · Stir-casting · Characterization

1 Introduction

Lightweight materials that possess exceptional mechanical and tribological properties are progressively gaining acceptance in numerous engineering applications such as the automotive, oil and gas, aerospace, and food industries [1]. Among these materials, Aluminum matrix composites (AMCs), a subclass of metal matrix composites (MMCs), have garnered attention due to their high strength-to-weight ratio, improved wear and corrosion resistance, and low coefficient of thermal expansion at a low production cost [2, 3]. To enhance the mechanical and tribological properties of aluminum alloys, researchers have explored the incorporation of various reinforcing materials such as graphite, boron carbide, (B_4C), alumina, silica, Zirconia, mullite, boron nitride, and titanium diboride (TiB_2), among others [4]. Singla et al. [5] demonstrated a significant improvement in the impact energy and hardness of Al-alloy composites by reinforcing with SiC particles. Similarly, Auradi et al. [6] observed a drop in the wear rate of Al6061 matrix composites upon the addition

✉ L. Osunmakinde, labaikaosunmakinde@yahoo.com | ¹Mechanical Engineering Department, Ladoke Akintola University of Technology, Ogbomoso, Nigeria. ²Mechanical Engineering Department, School of Science and Mathematics, Howard Payne University, Brownwood, TX 76801, USA.



of boron carbide (B_4C) and other ceramic particles. However, the high cost of ceramic particles serves as a drawback to their utilization as reinforcements, resulting in an elevated cost of Al-matrix composite production [7].

The primary selection criteria for Aluminium matrix composites (AMCs) revolve around their lightweight nature and high strength-to-weight ratios [8]. Consequently, considerable research efforts have been directed towards incorporating suitable reinforcements to achieve these objectives. The utilization of agricultural waste as reinforcements in Al-alloy has facilitated the development of affordable, lightweight aluminum matrix composites while preserving the desired mechanical and tribological properties [9, 10]. The availability of these inexpensive reinforcements encourages researchers to explore the creation and application of agricultural by-products as reinforcements, which are abundantly accessible at minimal or no cost. Satheesh and Pugazhavadivu [11] employed SiC and CSA in the double stair casting method to reinforce Al6061, Hima Gireesh et al. [12] utilized Aloe vera powder as reinforcement in Al-alloy, Alaneme et al. [13] employed GSA/SiC as reinforcer in aluminum alloy through the stir casting technique, and Praveen and Birru employed an agricultural by-product, bamboo leaf ash (BLA), for the development and characterization of a metal matrix composite. These studies all reported favorable particle recovery and dispersion within the composites, aiming to harness the cost-effectiveness of these materials while mitigating environmental concerns.

Various agro-wastes, such as breadfruit seed hull ash, bagasse ash, maize stalk, lemon grass ash (LGA), and bamboo stem ash, have been employed in different applications and documented [14–16]. Previous investigations have established that the presence of rice husk (RH), coconut shell (CS), and cassava peel (CP) contributes to environmental pollution, particularly in Africa, where these residues possess limited or negligible economic value. Research studies have indicated that in Nigeria alone 6.8 million tons of cassava peels, were derived from hand-peeled cassava tubers which accounted for 20% of the total. However, landfilling of these peels, leading to improper utilization of land resources, contaminates the air and affects human health [17]. By subjecting cassava peels to incineration at temperatures exceeding 700 °C for a short duration, cassava peel ash (CPA) is produced, characterized by a significant alumino-silicate content with minor amounts of MgO and Fe_2O_3 . Table 1 demonstrates that CPA predominantly comprises more than 70% combined alumino-silicate, MgO, and Fe_2O_3 . Furthermore, CPA exhibits potential as a temporary substitute in the manufacturing of concrete, polymer composites, particleboard, and biomass briquettes [17–19].

On a global scale, the annual production of rice husk (RH) reaches approximately 70 million tons, posing a significant ecological hazard due to its adverse effects on land areas and waterways, thereby impacting terrestrial and aquatic ecosystems [20]. Nigeria, in particular, witnesses substantial RH production, benefiting from its abundant availability and high silica content. During the milling of paddy rice, the resulting byproducts include bran, broken rice, and rice, accounting for approximately 78 to 79% of the total weight, while the remaining 22% to 21% constitutes the husk. In rice mills, the husk serves as a fuel for generating steam in the parboiling process. Notably, the husk comprises around 75% organic volatile matter, and upon combustion, the residual mass transforms into RHA, i.e., ash. In 1000 kg of milled paddy, approximately 220 kg of husk is generated, leading to the production of approximately 55 kg of RHA by the boiler when the husk is burned. RHA predominantly consists of over 90% SiO_2 as its principal constituent [20–22]. Coconut shell (CS) represents an agricultural by-product primarily found in tropical regions. Due to its limited economic value, CS is commonly utilized as a fuel source in boilers and furnaces. Through complete combustion of CS, coconut shell ash (CSA) is obtained, characterized by its prominent SiO_2 content, accompanied by significant amounts of Al_2O_3 , MgO, and Fe_2O_3 as complementary constituents. CSA exhibits a relatively low density of 2.05 g/cm³. However, if not adequately disposed of, CS poses a substantial environmental threat [23]. The presence of resilient and brittle phases in such waste materials renders them suitable for applications in low-cost, lightweight, and load-bearing composites. These composites find diverse uses in sectors such as sports equipment, the food industry, architecture, and automotive manufacturing.

Table 1 Elemental composition of Al-Si-Fe and chemical oxides in RHA, CSA, and CPA

Composition	Si	Cu	N	Fe	Mn	Ti	Al			
Al-alloy (%)	0.1	0.02	0.001	0.1	0.02	0.03	Bal			
Composition	SiO_2	Al_2O_3	Fe_2O_3	CaO	MgO	Na_2O	K_2O	SO_3	P_2O_5	C
RHA (%)	91.73	1.56	0.16	1.16	0.47	–	0.73	–	–	1.13
CSA (%)	45.46	15.65	12.73	0.75	15.81	0.42	–	–	0.02	–
CPA (%)	54.36	11.85	5.81	10.4	0.15	1.05	13.09	0.44	–	–

Empirical research has revealed that the choice and weight ratio of reinforcing elements have a substantial impact on the resulting composite's properties [24, 25]. A study conducted by Kaladgi et al. [26] employed stir casting to evaluate the effect of alumina and coconut shell ash on the mechanical characteristics of reinforced Al6061 composites. The results indicated that an increase in the weight fraction of reinforcing particles resulted in a concomitant increase in both hardness and tensile strength. Varalakshmi and Kumar [27] investigated to determine the impact of coconut shell ash on synthesized Al6061 composite, employing a stir casting route. The findings demonstrated that an increase in the weight fraction of the reinforcing particle resulted in an improvement in the ultimate tensile strength and hardness, despite a decrease in composite density. Prasad et al. [28] produced an Al composite with RHA and SiC particles using a double stir casting technique. The findings indicated an enhancement in hardness, yield, and tensile strengths, coupled with a decrease in composite density, as the weight fraction of reinforcing particles increased.

Although several studies have investigated the effects of single ash particle reinforcement on the properties of Al-based composites, research into the potential benefits of utilizing multiple agro-waste particles in a metal matrix particulate composite for engineering applications has been limited. Therefore, there is a need to explore the possibility of combining different ash particles as reinforcements to fabricate cost-effective composites with superior mechanical and physical properties. In light of this, the present study aims to investigate the impact of using a combination of RHA, CPA, and CSA as reinforcing agents on the properties of Al alloys.

2 Materials and methods

2.1 Materials and processing

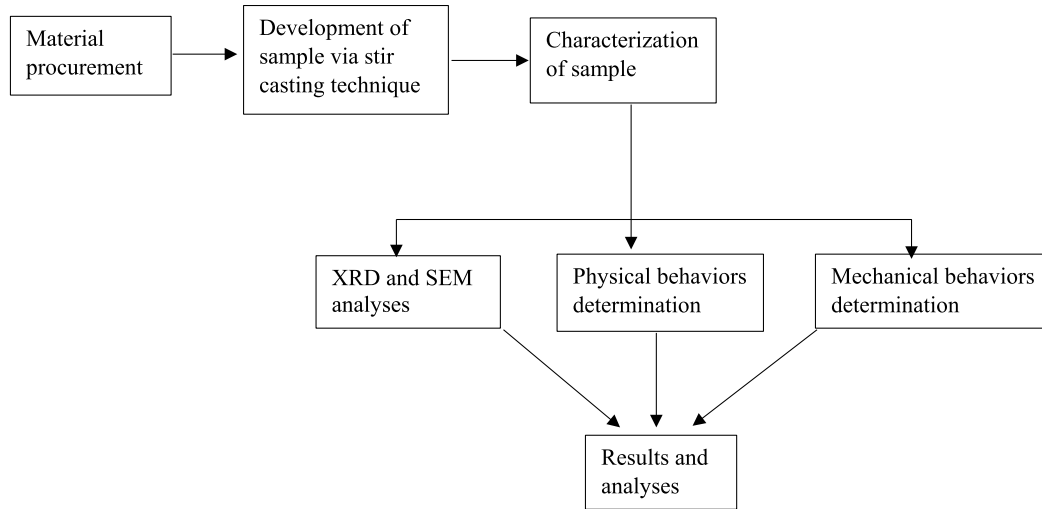
Locally produced rice husk, cassava peel, and coconut shell were obtained at Osogbo, Osun State, Nigeria. The agro-waste was thoroughly washed with distilled water and sun-dried for 5 days. The dried wastes were later valorized in a perforated drum for 12 h for complete calcination. The ash was subsequently sieved and stored in an air-tight container following the approach described by Alaneme et al. [29]. The aluminum (Al) powder, with a purity of 98%, was obtained from Loba Chemie PVT LTD India and served as the matrix for the composite. Table 1 provides a detailed overview of the elemental compositions of the pure Al powder and chemical oxides in the ash samples based on analysis. Accordingly, Al powder can be considered pure with some traces of Si, Cu and Mn. Also, RHA has about twice the amount of SiO₂ compared to CSA and CPA while CSA contains significant amounts of Al₂O₃, Fe₂O₃ and MgO compared to others.

2.2 Synthesis of the composites

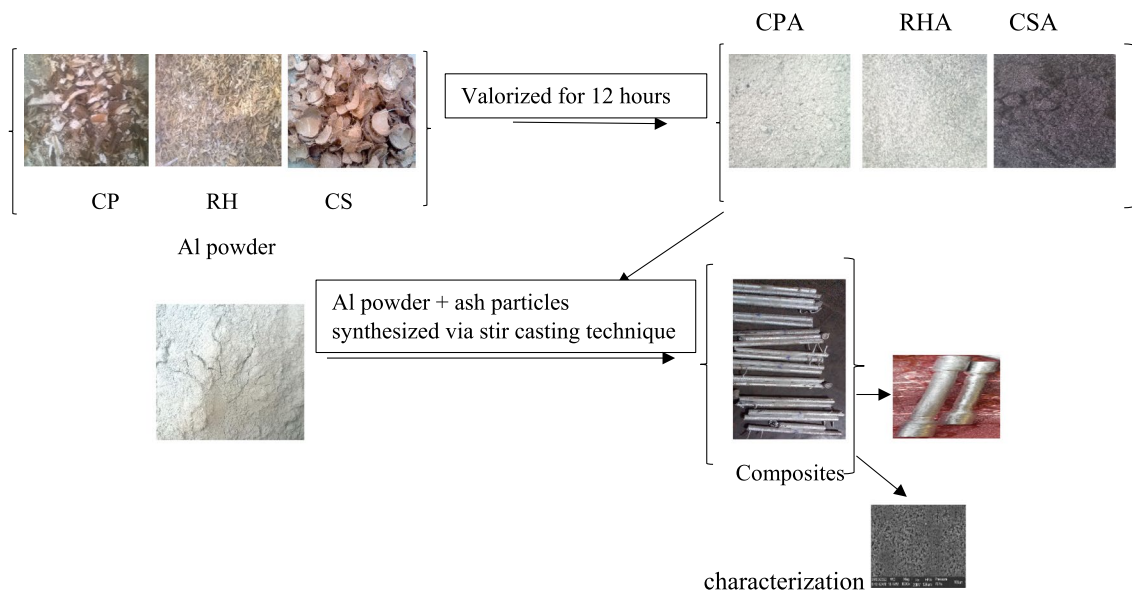
A cost-effective two-step stir-casting process was employed to fabricate Al composite. The amount of components for each sample was calculated following the experimental designs presented in Table 2. The pure aluminum powder was melted in a graphite crucible furnace at a temperature of 710 ± 20 °C [30, 31]. To remove moisture and improve wettability between the matrix and ash particles during melting, the ash particles were preheated at a temperature of 250 °C. Subsequently, the particles were introduced into the semi-solid melt while manually and rigorously stirred for a duration of 5–10 min to form a slurry. The slurry was superheated at 780 ± 30 °C and automatically stirred at 500 rpm for 8 min to achieve homogenous composition. Finally, the molten melts obtained from the process were poured into sand moulds and allowed to solidify (Fig. 1b).

2.3 Mechanical properties

Mechanical tests were carried out to evaluate the tensile strength, hardness, and impact resistance of the composites. Tensile tests were carried out using an Instron universal testing machine (UTM model 3369) according to ASTM 8 M-91 standard [32]. Dog-bone-shaped test specimens were made on a lathe machine and strained to fracture. The tensile characteristics were extracted from the stress–strain curves. The hardness tests were carried out using the Vickers hardness machine following ASTM E92 standard [33]. Three indents were made at different locations on each sample, and the average hardness value was calculated. The impact test was evaluated using the Hounsfield Izod impact machine (model no. 3816) adhering to the ASTM E691-14 standard for sample preparation and testing [34]. The test samples were made into 75 × 10 × 10 mm with V-notch at an angle of 45° to evaluate the as-cast composite's impact resistance (Fig. 1).



a: Schematic diagram of process map



b: Graphical image

Fig. 1 A Schematic diagram of process map

Table 2 Composite sample designation

Sample code	Composition
A ₀	Al-alloy
A ₁	Al-alloy + 15%wt CSA
A ₂	Al-alloy + 5%wt CSA + 5%wt RHA + 5%wt CPA
A ₃	Al-alloy + 15%wt CPA
A ₄	Al-alloy + 15%wt RHA

2.4 Physical property

The density and porosity of all samples were evaluated as a measure of physical characteristics. Equation (1) was used to calculate the density using the modified Archimedes approach while porosity values were obtained using Eq. 2 [35]. The mean density was estimated from three different measurements [36].

$$\rho_c = \left(M_1/M_2 \right) \rho_{\text{water}} \quad (1)$$

$$P = \frac{\rho_{\text{th}} - \rho_m}{\rho_{\text{th}}} \quad (2)$$

where ρ_c , M_1 , M_2 & ρ_{water} are the density of composite (g/cm^3), sample mass in the air (M_1), sample mass in water (M_2), and water density at room temperature ($1 \text{ g}/\text{cm}^3$). ρ_{th} and ρ_m are the theoretical and experimental densities, respectively.

2.5 Microstructural and XRD characterization

A JOEL-JSM 7600F Scanning Electron Microscope (SEM) with Energy-Dispersive X-ray Spectroscopy (EDS) capabilities was used to study the microstructures of the samples. The samples were ground, polished, and etched with Keller's reagent for 15–25 s before the microstructure examination was done. To identify the constituent phases present in the samples, a Rigaku D/Max-III C X-ray diffractometer was utilized. The instrument employed Cuka radiation, with an operating voltage of 40 kV and a current of 20 mA. Diffraction characteristics were obtained within a diffraction angle range of 2–50°, with a scan speed of 2°/min.

3 Results and the discussion

3.1 The X-ray diffraction results

Figure 2 shows the X-ray diffraction (XRD) spectra of the control and composite samples. Figure 2a demonstrates a cubic crystal structure exclusively composed of aluminum with a measured density of $2.72 \text{ g}/\text{cm}^3$. More oxides (SiO_2 , MgO , and intermetallic phases— Fe_3Si , Al_6Fe) are observed in the composites as shown in Figs. 2b–e indicating the presence of silica, alumina, ferric oxide, and magnesium oxide in the reinforcements (RHA, CSA, and CPA) as earlier observed (Table 1). The reaction between silica and ferric oxide produced Fe_3Si while the reaction between ferric oxide and aluminum gave Al_6Fe , both of which are intermetallic phases that are known to strengthen composites. This observation aligns with the findings of Aigbodion and Ezema [37], who reported a reaction between SiO_2 and MgO resulting in the formation of MgSiO_4 , without detrimental compounds such as Al_4C_3 being detected in the composites synthesized with A365 alloy reinforced with PKSanp. The analysis shows that agro waste ash mentioned above contains these oxides. Al_4C_3 adversely affects the mechanical and corrosion properties of composites, however, it was absent in the synthesized composites. In a related study by Atuanya et al. [38], XRD characterization of aluminum composites fabricated with breadfruit seed hull particles indicated the formation of Al_6Fe , Fe_3Si , and $\alpha\text{-Al}$, suggesting the involvement of the reinforcement materials in the composite. This is in agreement with the analysis highlighted in this study, which shows that interaction has occurred between the reinforcement and matrix. Despite the absence of Al_4C_3 , the XRD spectrum of the study's composites shows that interactions between the matrix and reinforcements had occurred.

3.2 Samples' microstructure

The SEM micrographs of the samples are shown in Fig. 3. Pure Aluminium exhibits a dendritic structure (Fig. 3a), but after reinforcing particles (RHA, CSA, and CPA) were added, the dendritic structures were pinned down and eventually vanished. Figures 3b–e show the representative micrograph of the monolithic reinforced and hybrid reinforced composites respectively. The ash particles were observed to be evenly dispersed within the composites with no region in the composites being left out. Furthermore, neither pores nor cracks were observed. This shows the effectiveness of the

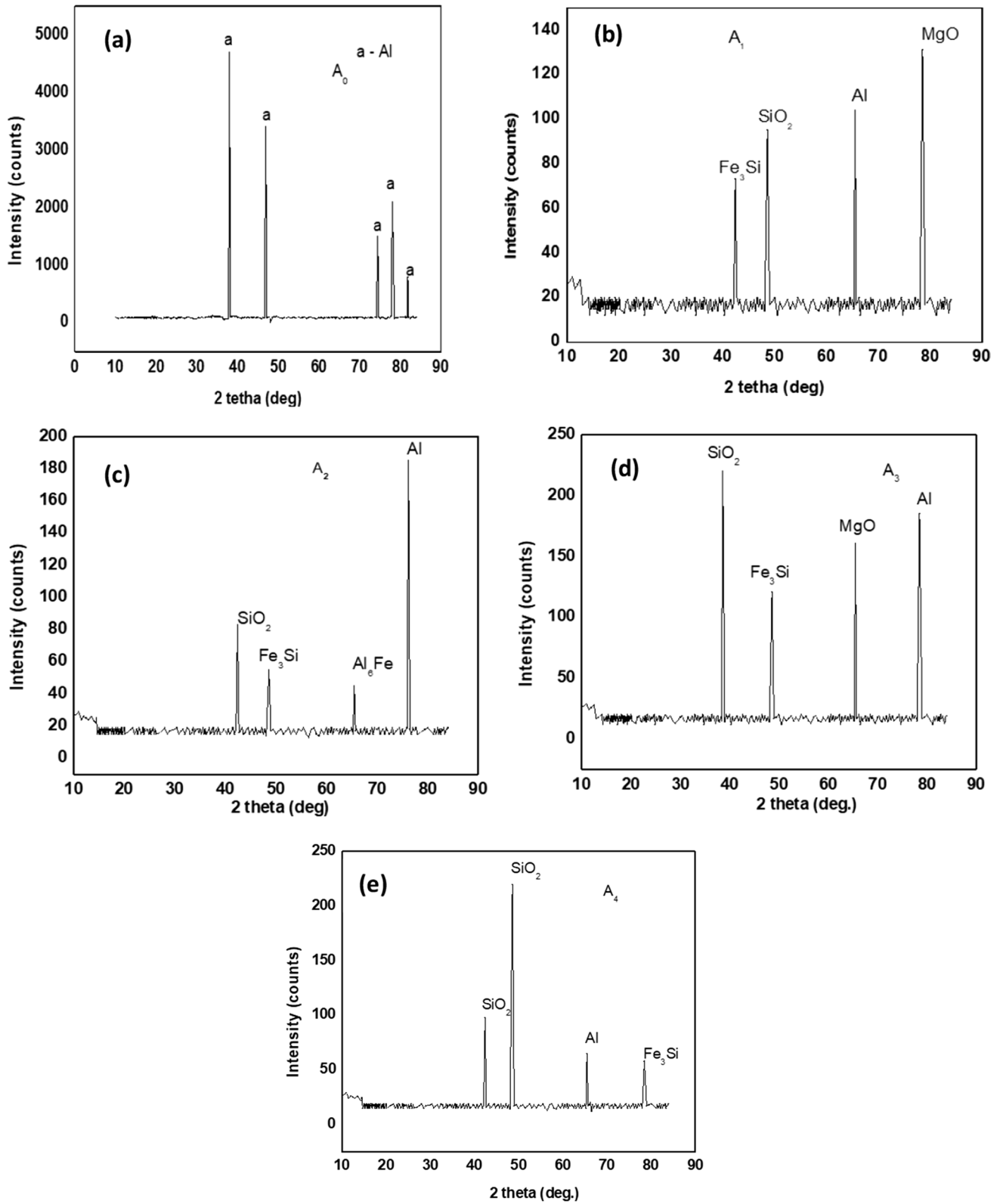


Fig. 2 XRD spectra for samples **a** A₀ **b** A₁ **c** A₂ **d** A₃ **e** A₄

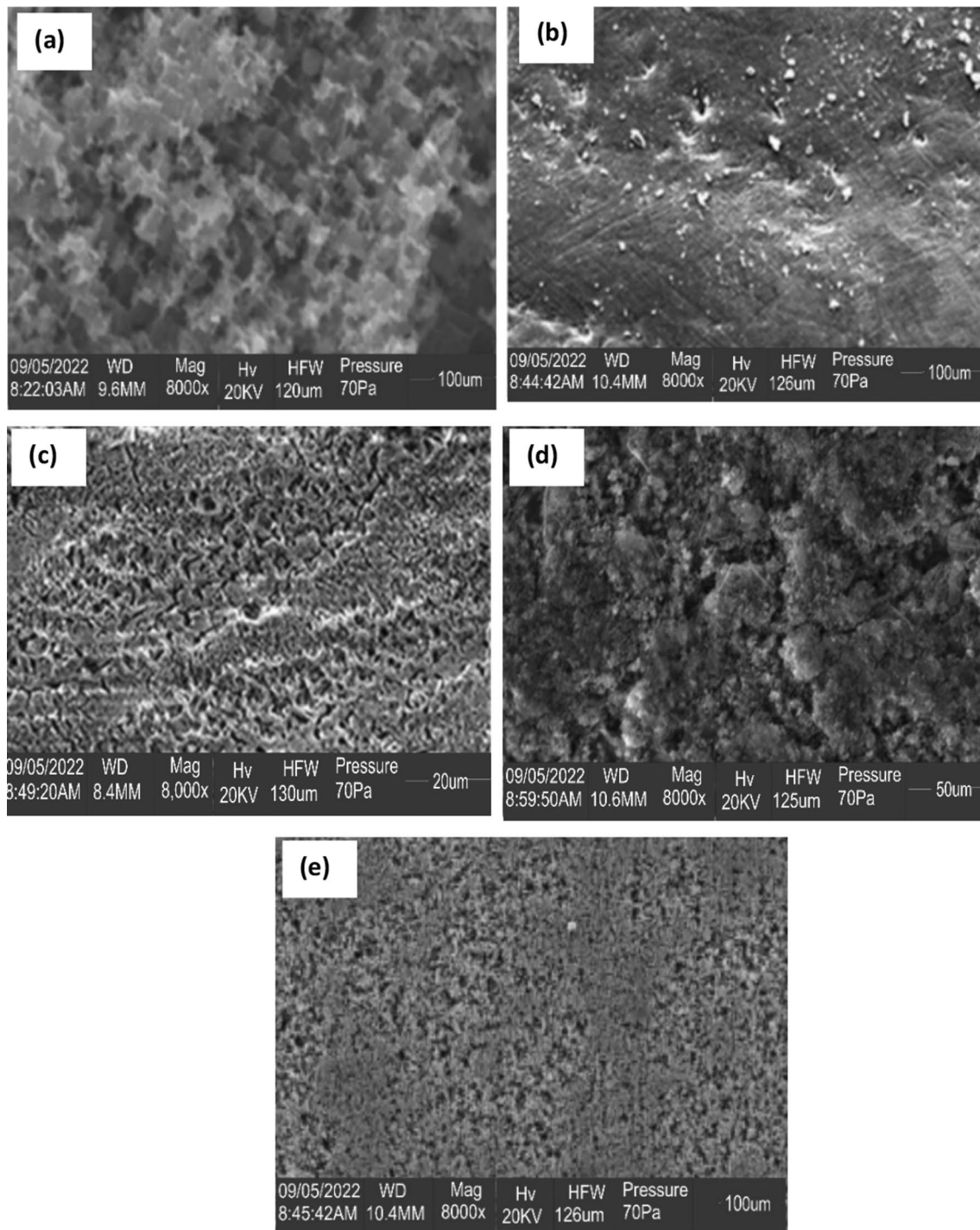


Fig. 3 SEM images of samples **a** A₀, **b** A₁, **c** A₂, **d** A₃, **e** A₄

double stair casting technique in relieving the surface tension between the Al matrix and reinforcing particles, resulting in a distinct interfacial appearance between the reinforcement particles and matrix [29, 30]. This affirms that the double stir casting technique is efficient for the production of the composite. The space between the matrix and the reinforcing ash is concurrent which indicates the homogeneity of the ashes in the composites.

However, the particles were not seen being clustered in a zone therefore the particles and the matrix were not agglomerated, because of the optimum stirring employed during the casting process. The dark parts in the composites are the ceramic content of the ashes scattered all around the composites. At 15%wt. ash, minute level of porosity was seen in

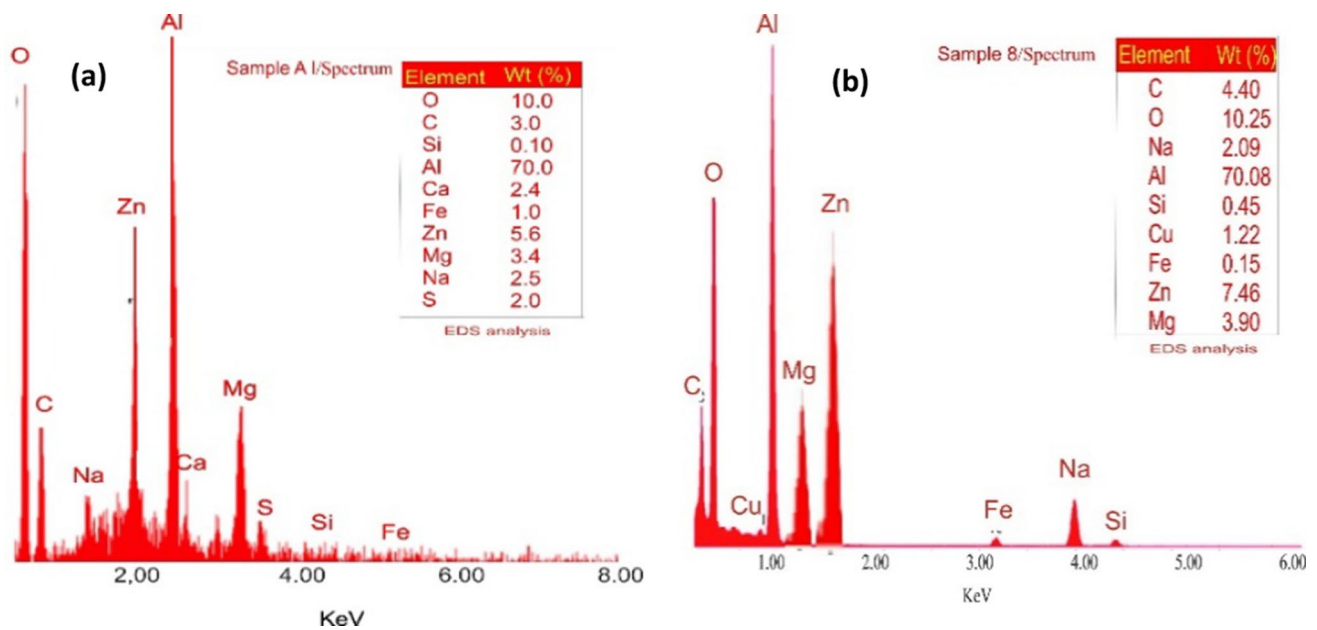
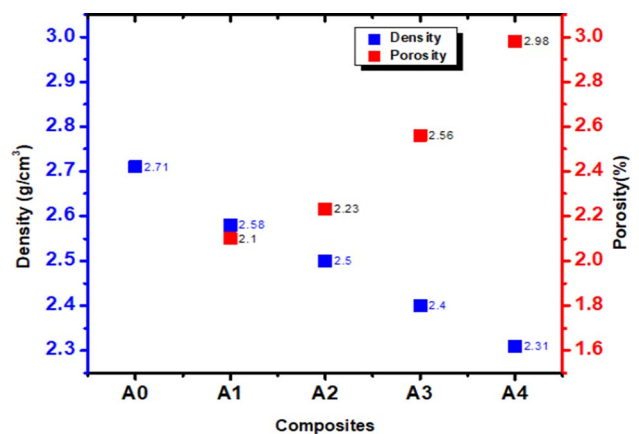


Fig. 4 EDX analysis of samples a A₀ b A₁

Fig. 5 Graph showing the porosity and density of composites made with various ash particles



the composite structure because of good interfacial bonding and wettability between the matrix and reinforcement particles. This was at par with composites synthesized from Al-4.5%Cu matrix-alloy reinforced with BLA particles as described by Praveen and Anil [39]; AA6061 matrix-alloy reinforced with RHA particles described by Dinaharan et al. [40]; and Al-Mg-Si matrix-alloy reinforced with hybrid particles SiC-CPA as reinforcement [41]. All reported similar phenomena with no cracks which further confirms the low porosity value observed in the representative SEM images, and particles were fairly well dispersed in the composites with good particle retention.

The EDS profiles (Fig. 4) of the matrix and composite show peaks of aluminum (Al), silicon (Si), iron (Fe), oxygen (O₂), and magnesium (Mg) which confirm the presence of (Al, Fe, Mg, and Si) as major elements in the matrix with capacity of reacting to form alumina (Al₂O₃), silica (SiO₂), ferric oxide (Fe₃O₂), and MgO in the composites. These compounds are fundamental constituents of the reinforcing ashes.

3.3 Density and porosity of the samples

The density, and percentage porosity of control sample and composite samples, are shown in Fig. 5. which reveal a significant impact of the added reinforcements. The density of the Al-matrix alloy was measured as 2.71 g/cm³, which is 14.76% higher than the density of sample A₄ containing Al-alloy/15%wt RHA, whose density was measured as 2.31 g/cm³. The addition of 15%wt CSA, and 15%wt CPA resulted in a 4.78%, and 11.44% decrease in the composite's density

respectively, while the incorporation of 5%wt CSA + 5%wt RHA + 5%wt CPA led to density reduction of 7.75%. The density reduction in each composite confirmed that the agro-wastes ash particles density is less compared to aluminum alloy density. Therefore, RHA, CSA, and CPA particulates lowers the density of fabricated composites. The density of CPA is 1.70 g/cm^3 [41]; the density of CSA is 2.05 g/cm^3 [42]. Findings by Alaneme et al. [29] demonstrated that the application of rice husk ash (RHA) in a hybrid Al–Mg–Si matrix composite reinforced with SiC reduced the composite density. The decrease in density was in connection with the added RHA particulates. Praveen and Anil [39] also reported a density reduction in Al–4.5%Cu composite reinforced with bamboo leaf ash, the reduction in density of the composites was attributed to the lower density of the ash. Additionally, Satheesh et al. [11] observed a decrease in the density of the Al6061–SiC hybrid composite with the incorporation of coconut shell ash (CSA).

The percentage porosity of the fabricated composites increased to 2.98% as the reinforcing ash was changed at 15%wt, which demonstrated the presence of small voids within the fabricated composites. According to Alaneme et al. [3], the highest permissible porosity in cast MMCs must not be higher than 4%. By limiting friction at the interface between the Al matrix and reinforcements, the percentage porosity of the manufactured composites falling within the range further proves the efficiency and dependability of the double stair casting method. Additionally, by allowing trapped air bubbles in the slurry to escape during processing, this casting technique lowers porosity [41, 43]. As observed in Fig. 5. Sample A₄, with the highest porosity, exhibits the lowest density, while sample A₀, with the least porosity, demonstrates the highest density. This observation aligns with the findings of Sasank et al. [44]. A similar study where Al6063 was reinforced with PKSA and SiC hybrid particulates by Ikubanni [1] revealed that the percentage porosity of the synthesized composites was less than 2.5%. This is within the acceptable limit since it is less than 4% which is recommended for cast MMCs. The physical properties obtained in this study indicate the potential for producing lightweight AMCs by utilizing multi-agro-waste ash as reinforcement in metal matrix composites. Such lightweight composites could find applications in automobile spare parts production such as cylinder liners and pistons among others.

3.4 Hardness, tensile strength, and impact energy of samples

Figures 6, 7 and 8 provide insight into the influence of reinforcements on the hardness, tensile strength, and impact energy of the samples. The hardness of the composites exhibited improvements of 14.24%, 21.38%, 28.06%, and 64.27% for samples A₃, A₁, A₄, and A₂, respectively, compared to the Al-alloy (see Fig. 6). The hardness changes as the ash particles change in the composites. The increase in hardness can be attributed to the presence of hard and brittle phases of the reinforcing particles in the malleable and soft phases of matrix material [29, 30]. Additionally, the hard and brittle phases of the reinforcement particles (as listed in Table 1), including SiO₂, MgO, Al₂O₃, and Fe₂O₃, which are constituent of RHA, CSA, and CPA, changed as the ash particles were changed and therefore enhanced composite hardness. The addition of 15%wt ash particles increases the surface area of reinforcement, leading to a reduction in matrix grain size, by increasing the volume of precipitated phases with associated plastic deformation resistance perhaps creating high dislocation density around the particle–matrix interface, therefore, improved the composite hardness. Same report was accredited to Hassan and Aigbodion [45] that reported higher hardness base on the presence of ceramic particles in the ESA reinforced composite against virgin alloy. Agbeleye et al. [46] reported similar effect when they reinforced

Fig. 6 Plotted hardness of fabricated composites

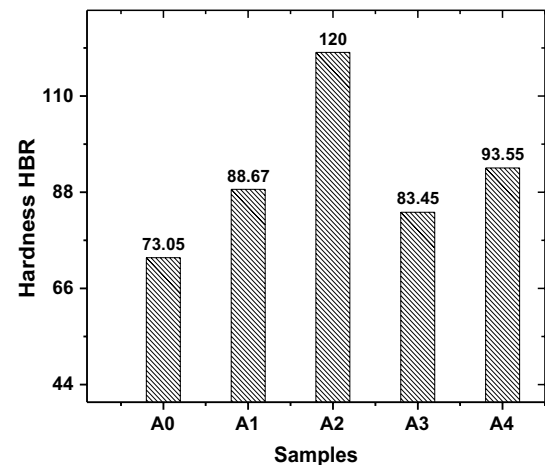


Fig. 7 Plotted Tensile strength of fabricated composites

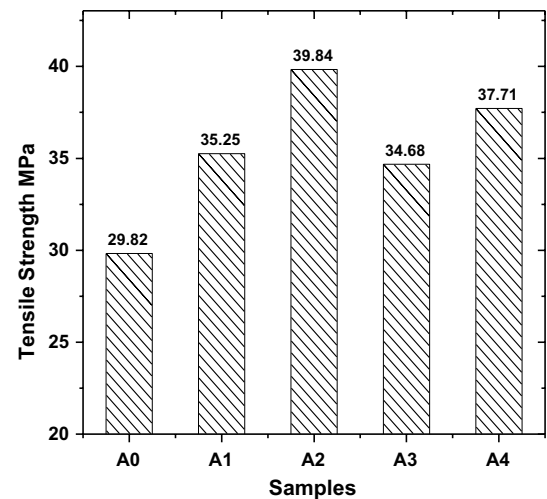
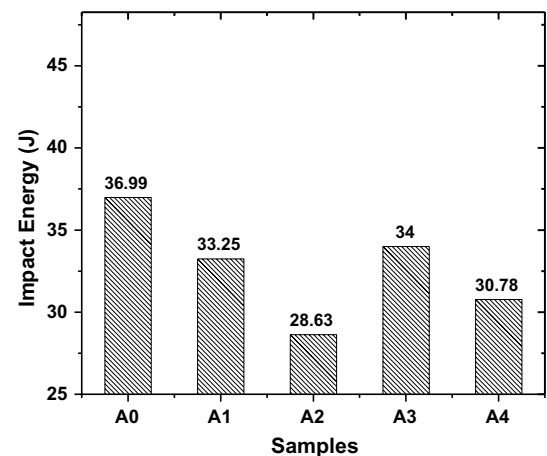


Fig. 8 Plotted impact energy of fabricated composites



AA6063 with clay. The slight difference in the hardness of synthesized composites was a result of the inconsistency of hard and brittle reinforcing oxides of each ash when compared, which significantly affects the load transfer mechanism at the particle matrix-particles interface. This observation aligns with Praveen and Anil [39], who demonstrated that the addition of bamboo leaf ash increased hardness and reduced the average grain size of the aluminum composite. The denser grain boundary line observed in the composites with higher quantities of reinforcement increases the dislocation density at the particle–matrix interfaces, resulting in an increase in plastic deformation resistance on the composites. This put RHA ahead of other agro-waste ash. This could be a result of more brittle and hard phases in the reinforcement used. This observation aligns with the studies conducted by Ikubanni et al. [1] and Praveen and Anil [39], and Madaskson et al. [47]. Agbeleye AA et al. [46] also corroborated the effect of clay on aluminum composites reinforced with clay for brake disc rotor applications. They explained that the application of reinforcements at 15%wt increases the composite's hardness and tensile strength but drops as the reinforcement percentage increases further. Previous research has shown that the presence of intermetallic compounds or phases in aluminum composites, such as $MgSiO_4$ and Fe_3Si , can greatly enhance hardness [21, 30, 36]. The results obtained in this study suggest that the developed composites can be suitable for lightweight applications where moderate hardness is required, such as sports equipment and architectural works.

The tensile strength samples A₃, A₁, A₄, and A₂ demonstrated an increase of 16.03%, 18.21%, 26.46%, and 33.60%, respectively, compared to the base alloy (see Fig. 7). However, this depicts the enhancement power of each ash based on their elemental compositions. The reaction and production of intermetallic phases, as well as the uniform distribution of hard and brittle phases within the ductile phase of the Al alloy, contribute to the influence of reinforcements on the tensile strength of the composite. According to Ikubanni et al. [1] enhancement in the tensile strength of hybrid composite reinforced with SiC and PKSA occurred as the PKSA incorporation increases in the base alloy. The addition of brittle and hard components from the ash particles (RHA, CSA, and CPA) improved the composites' tensile strength.

Praveen and Anil [39] reported an increase in the tensile strength of composite as bamboo leaf ash variation increased in the Al-4.5Cu alloy. Furthermore, the ability of the composites to transfer more loads as the reinforcing particles were added between the particle–matrix interface, strengthened the composite more thereby enhanced the tensile strength of the composites. This shows a correlation between hardness and tensile strength. The combined ash has more hard and brittle phases and gives the highest tensile value with more loads being transferred from the matrix into particles at their interface. Dinaharan et al. [40] revealed that interfacial bonding between matrix alloy and RHA particle was strong hence more load was transferred from the matrix into the particles at the particle–matrix interface during loading. Therefore, enhanced the composite better. Moreover, the morphological analysis of the synthesized composites revealed that the grain refinement caused by the reinforcement in the composites compared to base alloy improved tensile strength by reducing interparticle distance however, enhanced more particle interaction. The enhancement principles are discussed as follows.

Praveen and Anil revealed that a uniform dispersion of reinforcing particles throughout the Al-alloy matrix facilitates the Orowan mechanism into display during tensile loading creating a strong bond between the particles and the matrix, leading to enhanced tensile strength [39]. Furthermore, the inclusion of reinforcing materials refined composite grain size compared to matrix grain size therefore improved tensile strength through Hall–Petch equations [48]. While, the difference in the coefficient of thermal expansion between the matrix and the reinforcing material generates high dislocation density at the particle–matrix interface and inhibits the free flow of dislocation movement hence strengthening the tensile strength. The observed strengthening of the composite samples can be attributed to load transfer mechanisms at the interface between the base alloy and the reinforcing particles. This phenomenon involves the effective transfer of mechanical stresses and the creation of plastic deformation barriers within the composite structure. Consequently, the tensile characteristics of the composite are significantly influenced by the presence of RHA, CSA, and CPA particles [1, 7, 12, 15]. Among the composites with 15wt% reinforcement, composite A₂ exhibited the highest tensile strength and hardness, followed by A₄, A₁, and A₃, respectively, compared to virgin Al-alloy. This aligns with Ikubanni et al. [1]. The addition of these particles as reinforcement in aluminum matrix generates lightweight materials with improved strength and hardness which are useful in automobiles (pistons, connecting rods, cylinder liners) and architecture.

The impact energy, as demonstrated in Fig. 8, exhibited a decrease of 8.08%, 10.11%, 16.79%, and 22.60% for samples A₃, A₁, A₄, and A₂ respectively, compared to the virgin matrix (Al-alloy). The impact test reveals how brittle the reinforcing components are. Due to the brittleness of the reinforcing particles, the impact energy of each composite created reduced accordingly. This shows that the reinforcements impaired the toughness of the composites differently, the RHA particle has the least toughness, followed by CPA while, CSA has the highest toughness. This could be traced to the presence of ceramic particles (SiO₂) in the ashes, the silica percentage in RHA is the highest followed by the one in CPA while CSA is least (see Table 1). This assertion is elaborated with Al-alloy reinforced with hybrid particles of CSA and SiC, as the variation of CSA increases in the composites, the impact energy decreases [49]. Similarly, Hassan and Aigbodion developed Al-Cu-Mg composites reinforced with eggshell ash and reported similarly that an application of eggshell ash reduced the impact energy of the synthesized composites [45]. Moreover, the test revealed that the elastic property of the matrix material varies proportionally with the application of reinforcing particles due to the inelastic properties of these reinforcements. The particles impaired the composite's impact energy differently under sudden loading due to the inherent brittleness of each ash particle. Therefore, the ability of the composite to absorb energy diminished faster in composite A₂ than in the rest. However, the outcomes are within the standard level [11, 45, 49].

4 Conclusions

The aluminum alloy was subjected to reinforcement with varying weight percentages of coconut shell ash (CSA), rice husk ash (RHA), and cassava peel ash (CPA), namely 15wt% CSA, 15wt% RHA, 15wt% CPA, and 5wt% RHA + 5wt% CSA + 5wt% CPA. The key findings of the study can be summarized as follows:

- The composite exhibited optimal tensile strength and hardness when reinforced with 5wt% RHA + 5wt% CSA + 5wt% CPA, reaching values of 39.84 MPa and 120 HBR, respectively. However, the composite displayed reduced impact energy at this particular level of reinforcement. This indicates that the composite becomes harder and brittle with a reduced impact energy of 28.63 J. The obtained results from (A₁, A₃, and A₄) point out that the aforementioned agro-wastes are potential reinforcing materials which aid development of lightweight composite with good strength-to-weight ratio for various modern engineering applications at reduced production cost.

- The difference in the density values and chemical oxides of each reinforcing particle determined the physico-mechanical properties of the fabricated composites as reinforcing particles were added. The percentage variation in the density of synthesized composites (A_1 , A_2 , A_3 , and A_4) are 11.44%, 7.75%, 4.78%, and 14.76%, this shows that the application of RHA particles as reinforcement gave least dense composite compared to CPA and CSA.
- Compared to pure Al-alloy, the density result of synthesized aluminum matrix composites is dependent on the reinforcing particles. The presence of porosity within the composites was indicated by discrepancies between the theoretical and experimental density values.
- The composites contained a variety of substances, including silica (SiO_2), magnesium oxide (MgO), (Fe_3Si), and (Al_6Fe) according to the XRD spectrum. These oxides and intermetallic phases facilitated the composites' hardening and strengthening. The presence of Fe_3Si and Al_6Fe in composite A_2 enhanced its mechanical properties over others hence, could find application in automobile engineering. The composite sample A_2 was the best-synthesized composite among others.
- Scanning electron microscopy (SEM) analysis demonstrated a well-dispersed arrangement of the reinforcing materials within the composite, showcasing a clean interface between the matrix and the reinforcement particles.

Acknowledgements Not applicable.

Author contributions The research idea was conceptualized by OL, ATB, and AAP. OL provided the necessary materials for the research and conducted the sample preparation. Laboratory experiments on the prepared samples were carried out by OL and AAP to obtain the required data. Morphological examinations were performed by ATB and AAP. Data analysis was conducted by OL, who also took the lead in writing the initial manuscript. Scientific discussions regarding the manuscript involved contributions from OL, ATB, AAP, and DMO.

Data availability This will be made available upon request.

Code availability This will be made available upon request.

Declarations

Ethics approval and consent to participate Not applicable.

Competing interests The authors declare no competing interests.

Open Access This article is licensed under a Creative Commons Attribution 4.0 International License, which permits use, sharing, adaptation, distribution and reproduction in any medium or format, as long as you give appropriate credit to the original author(s) and the source, provide a link to the Creative Commons licence, and indicate if changes were made. The images or other third party material in this article are included in the article's Creative Commons licence, unless indicated otherwise in a credit line to the material. If material is not included in the article's Creative Commons licence and your intended use is not permitted by statutory regulation or exceeds the permitted use, you will need to obtain permission directly from the copyright holder. To view a copy of this licence, visit <http://creativecommons.org/licenses/by/4.0/>.

References

1. Ikubanni PP, Oki M, Adeleke AA. A review of ceramic/bio-based hybrid reinforced aluminum matrix composites. *Cogent Eng.* 2020;7:1–19.
2. Baisane VP, Sable YS, Dhobe MM, Sonawane PM. Recent development and challenges in processing of ceramics reinforced Al matrix composite through stir casting process. *Int J Eng Appl Sci.* 2015;2(10):2394–3661.
3. Dwivedi SP, Saxena A, Kumaraswamy A, Sahu R. Synthesis and characterization of waste SAC-and RHA-reinforced aluminium-based composites. *Green Mater.* 2021. <https://doi.org/10.1680/jgrma.20.00042>.
4. Yigesu SB, Mahapatra MM, Jha PK. Influence of reinforcement type on microstructure, hardness and tensile properties of an aluminum alloy metal matrix composite. *J Minner Mater Charact Eng.* 2013;1:124–30.
5. Singla MD, Deepak D, Singh L, Chawla V. Development of aluminum based silicon carbide particulate metal matrix composite. *JMMCE.* 2009;8(6):455–67.
6. Auradi V, Rajesh GL, Kori SA. Mechanical behavior and dry sliding wear properties of ceramic boron-carbide particulate reinforced Al6061 matrix composites. *Trans Indian Ceram Soc.* 2016;75(2):112–9.
7. Parveez BMDA, Jamal N. Influence of agro-based reinforcements on the property of aluminum matrix composites. *J Mater Sci.* 2021;56:16195–222.
8. Prasad DS, Shoba C. Hybrid composites are a better choice for high-wear-resistance materials. *J Mater Res Technol.* 2014;3(2):172–8.
9. kanthavel, K, Sumesh, K.R and Saravanan K.P. Study of tribological properties Al/Al₂O₃ MoS₂ hybrid composites processed by powder metallurgy. *Alexandria Eng J.* 2014;55:13–7.

10. Baradeswaran A, Perumal AE. Study on mechanical and wear properties of Al7075 /Al2O3/graphite hybrid composites. *Compos Part B*. 2014;56:464–71.
11. Satheesh M, Pugazhivadiv M. Investigation on physical and mechanical properties of Al6061-silicon carbide (SiC)/coconut shell ash (CSA) hybrid composites. *Physica B*. 2019;572:70–5.
12. Hima Gireesh C, Durga Prasad KG, Ramji K, Vinay PV. Mechanical characterization of aluminum metal matrix composite reinforced with aloe vera powder. *Mater Today*. 2018;5:3289–97.
13. Alaneme KK, Bodunrin MO, Awe AA. Microstructural, mechanical and fracture properties of groundnut shell ash and silicon carbide dispersion strengthened aluminum matrix composites. *J King Saud Univ Eng Sci*. 2018;30:96–103.
14. Kulkarni PP, Siddeswarappa B, Kumar KSH. A survey on effect of agro-waste ash as reinforcement on aluminum base metal matrix composites. *Open J Compos Mater*. 2019;9:312–26.
15. Joseph OO, Babremu KO. Agricultural waste as a reinforcement particulate for Al metal matrix composites (AMMCs). *Rev MDPI Fibers*. 2019;7:33.
16. Adebisi AA, Maleque A, Ali MY. Effect of variable particle size reinforcement on mechanical and wear properties 6061Al-SiCp composites. *Comp Interfaces*. 2016;23:533–47.
17. Adesanya OA, Shittu LA, Adesanya RA. *Internet J Microbiol*. 2008;5(1):25–35.
18. Abyaz A, Afra E, Saraeyan A. Improving technical parameters of biofuel briquette using cellulosic binder. *Energy Sources Part A Recover Util Environ Effects*. 2020;00(00):1–12.
19. Stephen WK, Jackson WM, Millien KE, Genson ML, Joseph MW. Characterization of composite material from the copolymerized polyphenolic matrix with treated cassava peel starch. *Sci Direct*. 2020. <https://doi.org/10.1016/j.heliyon.2020.e04574>.
20. Saravanan SD, Senthilkumar M, Shankar S. Effect of particle size on tribological behavior of rice husk ash-reinforced aluminum alloy (AlSi10Mg) matrix composites. *Tribology Transactions*. 2013;56:1156–67.
21. Yevich R, Logan JA. An assessment of biofuel use and burning of agro-waste in the developing world. *Global Biogeochem Cycles*. 2003. <https://doi.org/10.1029/2002gb001952>.
22. Tiwari S, Pradhan MK. Effect of rice husk ash on properties of Al-alloys. A review *Mater Today Proc*. 2017;4:486–95.
23. Kumar A, Nirala A, Singh VP, Sahoo BK, Singh RC, Chaudhary R, Dewangan AK, Gaurav GK, Klemes JJ, Liu X. The utilization of coconut shell ash in production of hybrid composite: microstructural characterization and performance analysis. *J Clean Prod*. 2023;398:136494. <https://doi.org/10.1016/j.jclepro.2023.136494>.
24. Anestiev L, Lazarova R, Petrov P, Dyakova V, Stanev I. On the strengthening and the strength reducing mechanism at aluminium matrix composites reinforced with nano-sized TiCN particulates. *Philos Mag*. 2021;101:129–53.
25. Chawla N, Shen Y. Mechanical behaviour of particle reinforced metal matrix composites. *Adv Eng Mater*. 2001;3(6):357–70.
26. Kaladgi ARR, Rehman KF, Afzal A, Baig MA, Soudagar MEM, Bhattacharyya S. Fabrication characteristics and mechanical behavior of Al alloy reinforced with Al₂O₃ and CS particles synthesized by stir casting. *IOP Conf Ser Mater Sci Eng*. 2021;1057:12017.
27. Varalakshmi K, Kumar CK, K, Ravindra Babu, P and Ch Sastry, M.R. Characterization of Al6061-CSA MMCs using stir casting. *Int J Latest Eng Sci*. 2019;2:41–9.
28. Prasad DS, Shoba C, Ramanaiah N. Investigations on mechanical properties of aluminum hybrid composites. *J Mater Res Technol*. 2014;3:79–85.
29. Alaneme KK, Sanusi KO. Microstructural characteristics, mechanical and wear behaviour of aluminum matrix hybrid composites reinforced with alumina, rice husk ash, and graphite. *Eng Sci Technol Int J*. 2015;18:416–22.
30. Nithyanandhan T, Ramamoorthi R. Development of bamboo stem ash-Al-hybrid reinforced with Al₂O₃ produced by stir casting technique. *J Ceram Process Res*. 2021;22(4):369–76.
31. Edoziuno FO, Adediran AA, Odoni BU, Utu OG, Olayanju A. Physico-mechanical and morphological evaluation of palm kernel shell particulate reinforced aluminium matrix composites. *Mater Today Proc*. 2021;38:652–7. <https://doi.org/10.1016/j.matpr.2020.03.641>.
32. ASTM E 8M (1991). Standard Test Method for Tension Testing of Metallic Materials. (Metric), Annual Book of ASTM standard Philadelphia, 1991.
33. ASTM E92 (2003). Standard Test Method for Vickers Hardness of Metallic Materials ASTM International, West Conshohocken, PA 2003. www.astm.org.
34. ASTM E691–14 (2018). Standard test method for impact test of metallic materials ASTM international. American Society for Testing and Materials. 85.
35. Karthikeyan P, Pramanik S. Thermal fatigue cycle checks effect on physical and structural properties of H13 tool steels before and after heat treatments. *IOP conf ser Sci Eng*. 2020;912(5):05 2014.
36. Prasad DV, Shoba C, Ramanaiah N. Investigations of mechanical properties of Aluminum hybrid composites. *J Mater Res*. 2014;3:79–85.
37. Aigbodion VS, Ezema IC. Multifunctional A365 alloy/PKSAmp composites: microstructure and mechanical properties. *Defense Technol*. 2020;16:731–6.
38. Atuanya CU, Ibhadowe AOA, Dagwa IM. Effects of breadfruit seed hull ash on the microstructures and properties of Al-Si-Fe alloy/breadfruit seed hull ash particulates composites. *Results Phys*. 2012;2:142–9.
39. Praveen KB, Anil KB. Strengthening of mechanical and tribological properties of Al-4.5%Cu matrix alloy with the addition of bamboo leaf ash. *Results Phys*. 2018;10:360–73.
40. Dinaharan I, Kalaiselvan K, Murugan N. Influence of rice husk ash particles on microstructure and tensile behaviour of AA6061 Al matrix composites produced using friction stir processing. *Comp Commun*. 2017;3:42–6.
41. Oladayo O, Akinlabi O, Babatunde O. Influence of silicon carbide-cassava peel ash weight ratio on the mechanical and tribological characteristics of Al-Mg-Si alloy hybrid composites. *J Chem Technol Metall*. 2021;56(5):1082–8.
42. Reddy PV, Prasad PR, Krishnudu DM, Goud EV. An investigation on mechanical and wear characteristics of Al6063/TiC metal matrix composites using RSM. *J Bio-Tribo-Corros*. 2019;5:1–10.
43. Senthilkumar S, Saravanan SD, Shankar S. Dry sliding wear and friction behaviour of aluminum-rice husk ash composites using Tagushis technique. *J Compos Mater*. 2015;49:2241–50.

44. Sasank SP, Ajit KS, Srinivasa Rao P. Effect of particle size on properties of industrial and agrowaste-reinforced AMCs. *Mater Metal Mater Soc JOM*. 2021;73(7):2096–103.
45. Hassan SB, Aigbodion VS. Effect of eggshell on the microstructures and properties of Al-Cu-Mg/eggshell particulate composites. *J King Saud Uni*. 2015;27:49–56.
46. Agbeleye AA, Esezobor DE, Balogun SA, Agunsoye JO, Solis J, Neville A. Tribological properties of aluminum-clay composites for brake disc rotor applications. *J of King Saud Univ Sci*. 2020;32:21–8.
47. Madaskson PB, Yawas DS, Apasi A. Characterization of coconut shell ash for potential utilization in metal matrix composites for automotive applications. *Int J Eng Sci Technol*. 2012;4(3):1190–8.
48. Meenashisundaram GK, Mui Hoon N, Gupta M. Effect of primary processing techniques and significance of Hall-Petch strengthening on the mechanical response of magnesium matrix composite containing TiO₂ nanoparticles. *MPDI*. 2015;5(3):1256–83.
49. Poomesh M, Saldanha JX, Singh J, Pinto GM. Effect of coconut shell ash and SiC particles on mechanical properties of aluminum based composites. *Am J Mater Sci*. 2017;7:112–5. <https://doi.org/10.5923/j.materials.20170704.09>.

Publisher's Note Springer Nature remains neutral with regard to jurisdictional claims in published maps and institutional affiliations.